cal maps than currently exist. Similarly, marine geologists no longer ply the seas in a spiderweb of ship tracks, but now choose specific areas for detailed study of particular phenomena. Perhaps the most rewarding and the most useful result of plate tectonics was the recognition that processes that had seemed too difficult to study except qualitatively could, in fact, be analysed quantitatively with simple physical concepts replete with mathematics and meaningful uncertainties. Although continental tectonics has not had a revolution like plate tectonics, it has nevertheless progressed enormously in the past 20 years.

I am grateful to B. C. Burchfiel, P. C. England, J. A. Jackson, R. McCaffrey, D. P. McKenzie, S. Neustadtl and P. Tapponnier for critically reading earlier drafts of this manuscript and D. L. Frank for numerous retypings of it. R. Allmendinger, C. H. Jones, S. Kaufman, P. Tapponnier and R. I. Walcott kindly supplied original figures. I thank NASA and NSF for continued support.

1. Vine, F. J. & Matthews, D. H. *Nature* **199**, 947-949 (1963).
2. Hamilton, W. *Geol. Soc. Am. Bull.* **80**, 2409-2430 (1969).
3. Dewey, J. F. & Bird, J. M. *J. geophys. Res.* **75**, 2625-2647 (1970).
4. Atwater, T. *Geol. Soc. Am. Bull.* **81**, 3513-3536 (1970).
5. Bibby, H. M. *Geophys. J. R. astr. Soc.* **66**, 513-533 (1981).
6. Walcott, R. I. *Geophys. J. R. astr. Soc.* **79**, 613-633 (1984).
7. Molnar, P. & Tapponnier, P. *Science* **189**, 419-426 (1975).
8. Tapponnier, P., Peltzer, G. & Armijo, R. in *Collision Tectonics* (eds Coward, M. P. & Ries, A. C.) 115-157 (Geological Society, London, 1986).
9. Brace, W. F. & Kohlstedt, D. L. *J. geophys. Res.* **85**, 6248-6252 (1980).
10. Chen, W.-P. & Molnar, P. *J. geophys. Res.* **88**, 4183-4214 (1983).
11. Molnar, P. & Lyon-Caen, H. *Spec. Pap. geol. Soc. Am.* **218**, 179-207 (1988).
12. Molnar, P. & Tapponnier, P. *J. geophys. Res.* **83**, 5361-5375 (1978).
13. England, P. C. & McKenzie, D. P. *Geophys. J. R. astr. Soc.* **70**, 295-321 (1982).
14. Houseman, G. A. & England, P. C. *J. geophys. Res.* **91**, 3651-3663 (1986).
15. Vilotte, J. P., Madariaga, R., Dagnières, M. & Zienkiewicz, O. *Geophys. J. R. astr. Soc.* **84**, 279-310 (1986).
16. England, P. C. & Houseman, G. A. *J. geophys. Res.* **91**, 3664-3674 (1986).
17. Peltzer, G. & Tapponnier, P. *J. geophys. Res.* (in the press).
18. Tapponnier, P., Peltzer, G., Le Dain, A. Y., Armijo, R. & Cobbold, P. *Geology* **10**, 611-616 (1982).
19. McKenzie, D. & Jackson, J. *Earth planet. Sci. Lett.* **65**, 182-202 (1983).
20. McKenzie, D. & Jackson, J. *J. geol. Soc. Lond.* **143**, 349-353 (1986).
21. Nur, A., Ron, H. & Scotti, O. *Geology* **14**, 746-749 (1986).
22. Burchfiel, B. C. *et al. Geol. Soc. Am. Bull.* (submitted).
23. Zhang Peizhen *et al. Geol. Soc. Am. Bull.* (submitted).
24. Beck, M. E. *Am. J. Sci.* **276**, 694-712 (1976).
25. Luyendyk, B. P., Kamerling, M. J., Terres, R. R. & Hornafius, J. S. *J. geophys. Res.* **90**, 12454-12466 (1985).
26. Ron, H., Freund, R., Garfunkel, Z. & Nur, A. *J. geophys. Res.* **89**, 6256-6270 (1984).
27. Kissel, C. & Laj, C. *Tectonophysics* **146**, 183-201 (1988).
28. Nelson, M. R. & Jones, C. H. *Tectonics* **6**, 13-33 (1987).
29. Nicholson, C., Seeber, L., Williams, P. & Sykes, L. R. *Tectonics* **5**, 629-648 (1986).
30. Sonder, L. J., England, P. C. & Houseman, G. A. *J. geophys. Res.* **91**, 4797-4810 (1986).
31. Lamb, S. H. *Earth planet. Sci. Lett.* **84**, 75-86 (1987).
32. Jackson, J. *Nature* **334**, 195-196 (1988).
33. Anderson, R. E. *Geol. Soc. Am. Bull.* **82**, 43-58 (1971).
34. Armstrong, R. L. *Geol. Soc. Am. Bull.* **83**, 1729-1754 (1972).
35. Wernicke, B. *Nature* **291**, 645-648 (1981).
36. Miller, E. L., Gans, P. B. & Garing, J. *Tectonics* **2**, 239-264 (1983).
37. Davis, G. A. & Lister, G. S. *Spec. Pap. geol. Soc. Am.* **218**, 133-159 (1988).
38. Jones, C. H. *Tectonics* **6**, 449-473 (1987).
39. Davis, G. A. & Burchfiel, B. C. *Geol. Soc. Am. Bull.* **84**, 1407-1422 (1973).
40. Cheadle, M. J. *et al. Tectonics* **5**, 293-320 (1986).
41. Lemiszki, P. J. & Brown, L. D. *Geol. Soc. am. Bull.* **100**, 665-676 (1988).
42. Hadley, D. & Kanamori, H. *Geol. Soc. Am. Bull.* **88**, 1469-1478 (1977).
43. Humphreys, E., Clayton, R. W. & Hager, B. H. *Geophys. Res. Lett.* **11**, 625-627 (1984).
44. Panza, G. F. & Müller, St. *Mem. Sci. Geol.* **33**, 43-50 (1979.
45. Houseman, G. A., McKenzie, D. P. & Molnar, P. *J. geophys. Res.* **86**, 6115-6132 (1981).
46. Lyon-Caen, H. & Molnar, P. *J. geophys. Res.* **88**, 8171-8191 (1983).
47. Molnar, P. *Phil. Trans. R. Soc.* **A326**, 33-88 (1988).

ARTICLES

New semiconductor device physics in polymer diodes and transistors

J. H. Burroughes, C. A. Jones & R. H. Friend

Cavendish Laboratory, Madingley Road, Cambridge CB3 0HE, UK

Semiconductor devices have been made from polyacetylene, a conjugated polymeric semiconductor. The device operates in a novel way: charge is stored in localized soliton-like excitations of the polymer chain, which are introduced not by doping or photoexcitation but by the presence of a surface electric field. The formation of charged solitons changes the optical properties of the polymer, introducing optical absorption below the band gap. Combined with the processibility of the polymer, these new electro-optic effects may be exploited technologically in electro-optic modulators.

THERE is current interest in the possible use of 'molecular' organic materials as the active materials in electronic or optical devices, and this field is now designated 'molecular electronics'. But basic questions as to whether or not it is possible (or appropriate) to make use of modes of operation familiar in inorganic semiconductor science remain largely unanswered. Conjugated polymers are 'molecular' analogues of inorganic semiconductors[1], which exhibit high electronic mobilities when doped[2]. Despite the considerable progress made in the past decade towards an understanding of the electronic properties of conjugated polymers, there has been relatively little work on their use as the active component in semiconductor device structures. There are several reasons for this, the most important of which is that most conjugated polymers cannot be conveniently processed to the forms required in these devices. Most conjugated polymers are not readily soluble in easily handled solvents, and are infusible. This has severely limited the scope for construction of devices and those that have been reported in the literature show rather poor characteristics. Schottky and p-n diodes have been studied by several groups[3-6], and rectification ratios ($I_{forward}/I_{reverse}$) of up to a few hundred have been reported. There are also reports of field-induced conductivity measured in MISFET (metal-insulator-semiconductor field-effect transistor) structures[7,8].

A major advance in the control of the polymer processing is in the use of a solution-processible precursor polymer which can be converted to the conjugated polymer after processing. This was first demonstrated by Edwards and Feast[9] for the preparation of polyacetylene (the Durham route) and it is polyacetylene produced by this route that we have used in the present studies. We have made thin-film devices by spin-coating the precursor polymer, poly((5,6-bis(trifluoro-methyl)-bicyclo-[2,2,2]octa-5,7-diene-2,3-diyl)-1,2-ethenediyl), in solution onto the required substrate, followed by heat treatment to convert to the polyacetylene by elimination of hexafluoroorthoxylene[10-15]. As we discuss later, the films of polyacetylene prepared in this way are p-doped (possibly with catalyst residues at chain ends) to a level suitable for device applications ($\sim 10^{16} cm^{-3}$), and these dopants do not appear to be mobile under applied electric fields. We have not found it necessary, therefore, to dope the

© 1988 Nature Publishing Group

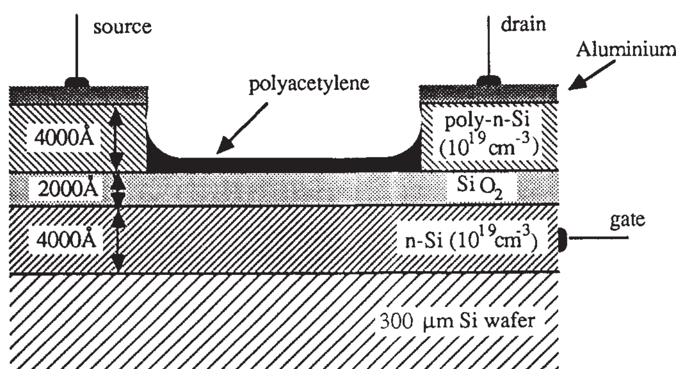

Fig. 1 Schematic diagram for a polyacetylene MISFET structure. Dimensions shown are to scale, except the channel width (20 μm) and length (1.5 m).

polymer further. We have investigated a range of unipolar devices: Schottky-barrier diodes, MIS (metal-insulator-semiconductor) structures and MISFETs. By careful control of the processing, with rigorous exclusion of oxygen, we have been able to get the device performance up to levels respectable enough to learn about the detailed functioning of the device. For the Schottky diodes we routinely measure rectification ratios of about 500,000, and for the MIS and MISFET structures we can demonstrate that the devices show 'textbook' formation of charge accumulation, inversion and depletion layers at the polyacetylene-insulator interface.

We did not expect charge storage in these devices to be in the band states as electrons and holes. It is established that there is a structural relaxation around charges present on the polymer chains, both when charges are added to the polymer chain through chemical doping, or separated following photoexcitation. For polyacetylene, the localized states are bond alternation defects, or solitons[16,17]. Charge injected into the polyacetylene in these device structures should also be stored in soliton states. The formation of a depletion layer in polyacetylene should remove the charged solitons introduced through extrinsic doping. The formation of an accumulation or inversion layer, however, provides a new means of charging the polymer chains. The clearest evidence for the formation of solitons in polyacetylene is the appearance of additional optical absorption below the band gap, associated with the vibrational and electronic excitations of the solitons[18]. For polyacetylene prepared by the Durham route the 'mid-gap' absorption feature due to transitions between the 'mid-gap' levels of the solitons and the band edges is seen at ~1.0 eV for chemically doped samples[13], and at 0.55 eV for photoexcited charges[15]. We expect, therefore, that 'charge injection' will change the optical properties of the polyacetylene in these devices; depletion should reduce the mid-gap optical absorption whereas accumulation or inversion-layer formation should introduce mid-gap states onto previously undistorted chains, increasing the mid-gap optical absorption. We find both qualitative and quantitative agreement with these theoretical predictions.

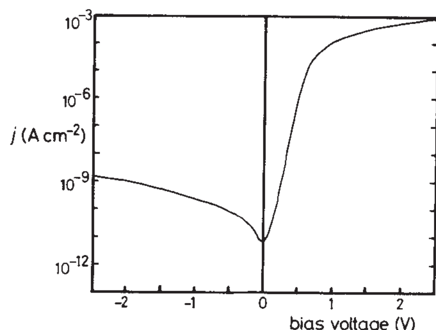

Fig. 2 Modulus of current versus voltage for a Schottky diode.

Fabrication

Thin films of polyacetylene were formed by spin-coating films of the Durham precursor polymer from solution in 2-butanone. Transformation of the precursor polymer to the *trans* isomer of polyacetylene was achieved by heating the film to 80 °C for 12 h. By adjustment of the concentration of the precursor polymer solution and the conditions for spin-coating, fully dense, coherent films of polyacetylene with thicknesses in the range 200 Å to 1 μm were readily produced. All fabrication and measurements involving the polyacetylene were carried out with rigorous exclusion of oxygen. A variety of device structures were fabricated and examples are given below. Note that most of these are arranged to allow passage of sub-band-gap light through the layers.

Schottky diodes. The multilayer structure used was built up with a wide-field spectrosil substrate, 200 Å gold, polyacetylene film (typically 1 μm), and a top contact of 200 Å aluminium. Gold forms an ohmic contact with p-type polyacetylene, aluminium the rectifying contact.

MIS diodes. Several configurations have been used. (1) Ultrapure silicon substrate (thickness 0.3 mm, $<10^{13}$ cm^{-3} charged impurities), 4,000 Å heavily phosphorus-doped ($>10^{19}$ cm^{-3}) silicon layer, 2,000 Å silicon dioxide (insulator layer), polyacetylene (typically 200–1,200 Å) and a top contact of 200 Å gold. (2) Wide-field spectrosil substrate, 200 Å gold, 1,500 Å poly(methyl-methacrylate) (insulator layer; spin-coated from dichloromethane solution), polyacetylene film (typically 200 Å), 200 Å chromium and 100 Å gold.

MISFET structures. (1) Gold source and drain contacts: n-doped silicon substrate (distributed gate electrode), 2,000 Å silicon dioxide, gold source and drain electrodes (thickness 500 Å, channel length 0.1 mm, channel width 75 mm), polyacetylene film (typically 200 Å). Similar source and drain contacts can also be deposited by evaporation onto the MIS diode (2) above. (2) Poly n-silicon source and drain contacts: the structure used is shown as Fig. 1.

Electrical characterization

Schottky diodes. The current density versus voltage characteristics for Schottky diodes constructed as above are shown in Fig. 2, in which log $|I|$ is plotted versus bias voltage for both forward and reverse biases. The ratio of forward to reverse current reaches a value of typically 5×10^5 at bias voltages of ~1.5 V. The usual parameterization for the variation of current density with bias voltage is $J=J_{sat}\exp(qV/nkT)$ for $V>3kT/q$, where n is the ideality factor, which for a 'perfect' diode is equal to 1. As seen in Fig. 2, $n\approx1.3$ at low forward biases. At higher forward biases the current is limited by the bulk resistance. In the thermionic emission model for conduction across the junction, the saturation current density, J_{sat} is given by $J_{sat}=A^*T^2\exp\{q\Psi/kT\}$, with A^* the effective Richardson constant (120 A K^{-2} cm^{-2} for an effective electron mass of one), and Ψ the barrier height[19]. By extrapolating from the linear region in Fig. 2, we estimate that $J_{sat}=4.4\times10^{-13}$ A cm^{-1}, and hence $\Psi=$ 1.28 eV. The reverse current does not appear to saturate, contrary to the prediction of the thermionic emission model; this is probably caused by the formation of a small interfacial layer between the polyacetylene film and the blocking contact[20]. The doping density may be obtained from the variation of the Schottky diode capacitance with reverse bias voltage, using the simple depletion model for the voltage dependence of the deple-

© 1988 Nature Publishing Group

tion width. In terms of the measured differential capacitance, C, this may be expressed as

$$\frac{1}{C^2}=\frac{1}{A^2}\left(\frac{2(\phi+V)}{\varepsilon_r\varepsilon_0 q N_A}\right)$$

where N_A is the acceptor concentration and ϕ is the built-in potential[19]. This relation is obeyed well for reverse bias, giving values of $N_A = 9\times10^{15}$ cm^{-3} and $\phi = 0.94$ V. We thus find that the electrical characteristics of the Schottky barrier between aluminium and polyacetylene indicate that the device is operating in the conventional way, whereby the depletion layer boundary moves under the influence of the applied bias voltage. We show later, however, that the charge depleted in the polyacetylene is stored in soliton states, rather than as holes in the valence band, in which case detailed modelling of the electrical properties using a conventional, rigid-band picture is inappropriate.

MIS structures. The MIS structure allows the possibility of band bending at the insulator-semiconductor interface through the Fermi level to produce a surface-charge layer which may be of the same carrier sign as the majority carriers (accumulation layer) or as the minority carriers (inversion layer)[21]. The formation of accumulation, depletion and inversion layers may be demonstrated through the relationship between the device capacitance and the bias voltage. The measured capacitance, C, is that of the series combination of the insulator capacitance, C_i, and the capacitance of the active region of the semiconductor, C_d, and is given by $C = C_iC_d/(C_i+C_d)$. Because C_d is large for the accumulation and inversion layers, C is equal to the geometric capacitance of the insulating layer, but falls to a lower value if the depletion layer moves. The capacitance versus bias voltage curve for a polyacetylene MIS structure is shown in Fig. 3. As expected, for negative gate voltages the capacitance tends to the geometric capacitance of the insulator, indicating the formation of an accumulation layer. The decrease in measured capacitance for positive voltages reveals the formation of a depletion layer. Saturation of the capacitance sets in for large positive biases, when the depletion layer extends across the polyacetylene film (estimated to be ~1,200 Å in thickness for this device).

MISFETs. A MISFET structure demonstrates that the charges at the polyacetylene-insulator interface in the MIS structure are mobile: source and drain contacts allow measurement of the conductance of the surface charge layer. Figure 4*a* shows results for a MISFET fabricated with gold source and drain contacts, for which the channel current, I_{DS}, is plotted against drain voltage, V_{DS}, for different gate voltages, V_{GS}. The channel current increases with negative gate voltage and saturates for large V_{DS} because of pinch-off of the channel near the drain electrode. Since the source and drain electrodes form ohmic contacts with the polyacetylene, we expect majority carrier injection from the electrodes into the polymer. The device is thus operating by modulation of the accumulation layer at the semiconductor-insulator interface. The channel conductivity for this structure could be modulated by a factor of about 2,000, from extreme depletion (full thickness of polyacetylene depleted) at $V_{GS} = +5$V to accumulation at $V_{GS} = -30$V. Formation of an inversion layer for large positive gate voltages is not expected to increase the channel conductance since the gold source and drain contacts are expected to form blocking contacts to the n-polyacetylene layer.

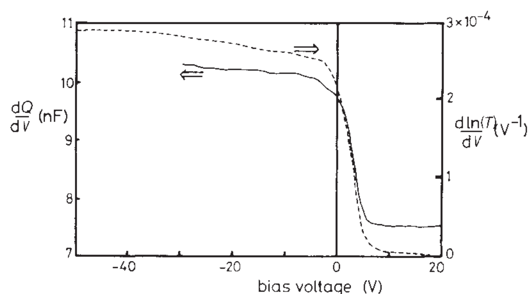

Fig. 3 The differential optical transmission, $\partial\ln(T)/\partial V$ at 0.8 eV (dashed), and differential capacitance, $\partial Q/\partial V$ (solid) versus bias voltage for the MIS structure. Measurements were made at 500 Hz and with an a.c. modulation of 0.25 eV.

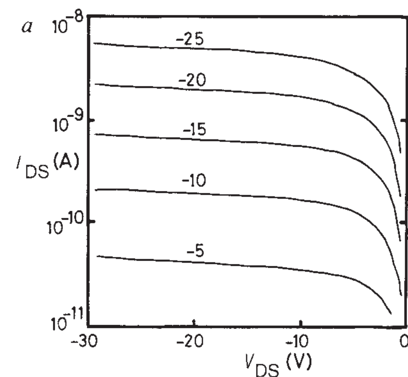

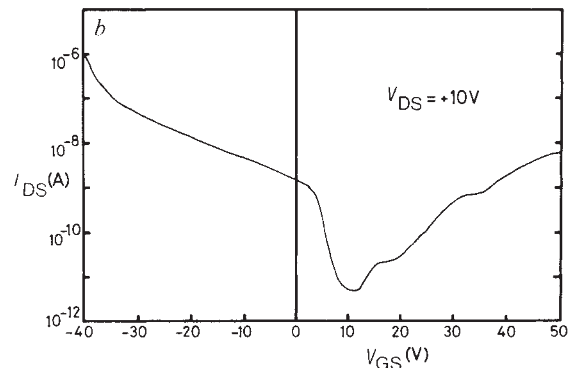

Fig. 4 *a*, I_{DS} versus V_{DS} at values of V_{GS} from −5 to −25 V, for a MISFET with gold source and drain contacts. *b*, I_{DS} versus V_{GS} at constant V_{DS} (+10V) for a MISFET with poly n-silicon source and drain contacts, as shown in Fig. 1.

The MISFET shown in Fig. 1 is constructed with n-silicon source and drain contacts, which are expected to make ohmic contacts to the n-polyacetylene layer. We thus expect to find enhanced channel conductance by formation of an n-type inversion layer for positive gate voltages. Figure 4*b* shows the variation of I_{DS} with V_{GS} at constant V_{DS}. The channel conductance has a minimum at $V_{GS} = +10$V (full depletion) and rises for gate voltages both more positive (inversion layer) and more negative (accumulation layer), with a maximum on/off ratio for this structure of 100,000 ($V_{GS} = -40$V to $+10$V). We see, therefore, the behaviour expected for positive bias, although the strong enhancement of the conductivity for negative bias indicates that the accumulation layer is still able to make good contact to the source and drain electrodes.

The MISFET structure provides a very convenient means of controlling the charge carrier concentration in the surface layer of the semiconductor. We have determined the carrier mobility from conductance measurements as a function of gate voltage, and find low values, typically 10^{-4} cm^2 V^{-1} s^{-1}. Similar mobilities are estimated for photogenerated carriers and for the extrinsic carriers in Durham polyacetylene (P. D. Townsend

© 1988 Nature Publishing Group

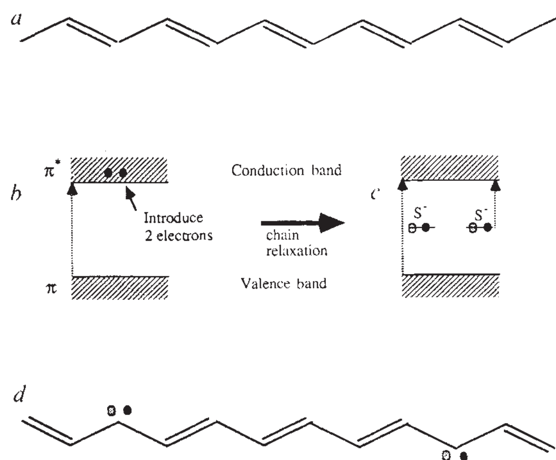

Fig. 5 Schematic representation of the formation of a pair of solitons on a polyacetylene chain. *a*, Undistorted chain; *b*, associated band scheme. The interband $\pi-\pi^*$ optical transition is shown as a dotted arrow. If two electrons are introduced into the conduction band of the chain as shown in *b*, the chain relaxes to the form shown in *d*, with a reversed sense of bond alternation in the centre of the chain separated by two solitons. Associated with the two solitons are non-bonding π states in the gap, created from one (doubly occupied) valence and one (empty) conduction band state. These two states (S) are doubly occupied, as shown in *c*, and each carries a negative charge. New optical transitions from the soliton level to the conduction band are indicated with a dotted arrow; the oscillator strength for the interband transition is weakened through the loss of the band states. A complementary picture holds for positive charge, which is accommodated as unoccupied solitons levels.

and R. H. Friend, to be published); we consider that the mobility-limiting process is the transfer of charge between chains.

Optical properties

As discussed earlier, charge in polyacetylene is stored in 'soliton' localized states, which are associated with non-bonding p_z mid-gap states. As a result, we expect to see a modulation in the optical properties of the active semiconductor region of these devices with applied bias voltage. The formation of a pair of negatively-charged solitons on a polyacetylene chain is shown schematically in Fig. 5.

Schottky diodes. An increase in the width of the depletion layer should remove charged soliton states thereby reducing absorption within the gap and increasing the absorption in the region of the $\pi-\pi^*$ transitions above 1.4 eV. The voltage-modulated transmission (VMT) spectrum between 0.4 and 1.8 eV is shown in Fig. 6. The positive signal for energies less than 1.4 eV shows that the transmission does increase for reverse bias voltages. The position of the electro-bleaching peak at 0.55 eV is in general agreement with photo-induced absorption experiments[15] on spin-coated Durham polyacetylene. The periodic structure in the modulated transmission spectrum below the band gap is due to the formation of interference fringes (modulation of the finesse of the Fabry-Perot etalon formed by the polyacetylene film). Electro-absorption is seen at energies greater than 1.4 eV, as expected if extra π- and π^*-band states are created at the expense of soliton states.

MIS and MISFET structures. For these structures we expect a decrease in the device transmission below the band-edge as the device is driven towards accumulation and new charged solitons are introduced onto the polyacetylene chains at the interface with the insulator. The VMT spectrum between 0.4 and 1.2 eV (Fig. 7*a*) shows a decrease in the transmission through the device for negative bias. The peak value of $\Delta T/T$, at 0.8 eV, is ~0.64%. If all the charge at the polymer-insulator interface is stored in soliton-like states then the VMT signal, $\partial \ln(T)/\partial V$, should scale with $\partial Q/\partial V$, the differential capacitance, as the bias voltage is varied. This is shown to be the case in Fig. 3, where $\partial \ln(T)/\partial V$ and the differential capacitance are both plotted against bias voltage. We have investigated the VMT response in a variety of structures, including the MISFET shown in Fig. 1. For this structure we find results similar to those in Fig. 7*a*, that is, the VMT response expected for both accumulation and inversion. It should be noted that the optical path for the MISFET is between the source and drain contacts, and that there is no 'back' electrode.

For the low areal soliton concentrations, N^a, found in the device structures, the modulation in transmission, $\Delta T/T$, can be expressed as σN^a, where σ is the optical cross-section for the dopant-induced mid-gap absorption. The determination of N^a is particularly simple for the MIS device driven into accumulation, for which $N^a = \varepsilon_r \varepsilon_0 V/qd$, where V is the bias voltage and d the insulator thickness. The value for $\partial \ln(T)/\partial V$ becomes constant for negative bias voltages (Fig. 3), as expected in this simple model. Typical results, such as those shown in Fig. 7*a*, give the magnitude of the optical cross-section at the peak in the mid-gap absorption as 1.2×10^{-15} cm^2, in very close agreement with the value measured from dopant-induced absorption[18]. We obtain similar agreement from analysis of optical modulation in the Schottky diode. Note that the maximum depth of optical modulation is fixed by the maximum value for N^a, which is determined for the MIS structure by the product $\varepsilon_r E_{max}$ for the insulator, where E_{max} is the dielectric breakdown field. For silicon oxide, the maximum value for N^a is $\sim 2\times10^{13}$ cm^{-2}, and the maximum value for $\Delta T/T$ is thus ~2.4%.

Besides the electronic transitions associated with the soliton state, there is extra infrared activity from new vibrational modes that couple to motion of the charged soliton along the polymer chain[22]. These are seen in both doping[13] and photoexcitation[15] experiments on unoriented Durham polyacetylene. Figure 7*b* shows the results from an FTIR experiment on an MIS structure, showing the difference in transmission for the MIS device biased between 0 and −50V with respect to the gate. There are three peaks: an absorption above 4,000 cm^{-1} (this is the low-energy side of the electronic absorption, as in Fig. 7*a*) and two sharp vibrational features at 1,379 and 1,281 cm^{-1}. We identify these as the two higher-frequency translation modes of the soliton. The value of 1,379 cm^{-1} lies between that measured for photo-induced charges, 1,373 cm^{-1} (ref. 15), and for dopant-induced charges, 1,410 cm^{-1} (ref. 13), and provides information about the chain conformation and degree of conjugation. We were not able to measure the VMT spectrum below 1,000 cm^{-1} because

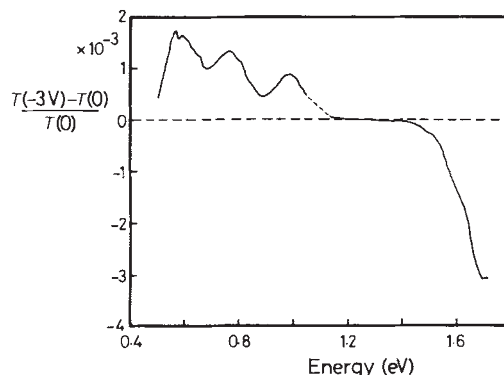

Fig. 6 Voltage-modulated transmission for a Schottky diode, $[T(V)-T(0)]/T(0)$, versus photon energy (E_p), with $V=-3$ V with respect to the blocking contact.

© 1988 Nature Publishing Group

of a very large absorption peak from SiO_2, and we were thus unable to observe the lowest-frequency, 'pinned' translational mode.

The results presented above are all obtained on structures with silicon dioxide as the insulator layer. It is important to demonstrate that these effects can be achieved with other insulators, and we have investigated several organic systems that can be readily formed as thin coherent films. Results on polyacetylene MIS structures, with spin-coated poly(methylmethacrylate) serving as the insulator, show similar behaviour, with an absorption band below the band gap, although the peak in absorption is at a lower energy, 0.55 eV.

Discussion

The formation of depletion, inversion and accumulation charge layers in a semiconductor device is restricted to semiconductors that are free of defects with energy levels within the semiconductor gap. Polymeric semiconductors are not obvious candidates since the structure is inherently disordered, with a large number of conformation defects (bends, twists) on the chains. But there are two principles common to conjugated polymers which run in their favour. First, there are no unsatisfied chemical bonds at the surface of the polymer, and we can expect that if the interface with the metal (Schottky diode) or insulator (MIS structures) is prepared in clean, oxygen-free conditions, we should avoid the problems with surface states well known for inorganic semiconductors. Second, defects on the polymer chain tend naturally to weaken the degree of π electron delocalization, and therefore to increase the π-π^* gap at the defect[11,13,15]. The electronic levels associated with the defect are thus removed from the semiconductor gap and play no active part in the device operation. This principle is of particular importance here since the unoriented films of Durham polyacetylene we have used are known to have straight-chain sequences of no more than 20 or so carbon-carbon bonds[10-15].

Optical spectroscopy reveals that charge storage in depletion, inversion or accumulation layers in these polyacetylene devices is not in band states (as with conventional semiconductors) but in soliton-like mid-gap states. For the depletion layer the chain deformation associated with these states is achieved by extrinsic doping. For accumulation and inversion layers, however, we have demonstrated a new means of putting charge onto the chains, in which the presence of the surface field forces charged soliton-antisoliton pairs onto previously undistorted chains, as shown schematically in Fig. 5.

Modulation of the optical properties by control of the charged-soliton density with the voltage applied across the device provides a new and powerful spectroscopy for investigating the electronic structure of the active region in these semiconductor devices. By comparison of the variation of differential transmission at mid-gap ($\partial \ln(T)/\partial V$) and the differential capacitance ($\partial Q/\partial V$) with bias voltage, we have shown that there is a direct correspondence between the two quantities and that therefore all charges at the interface are accommodated on polyacetylene chains in soliton-like states. From the spectrally resolved electronic and vibrational absorption features, we can also learn much about the detailed electronic structure of those polymer chains at the interface on which the charge is stored; we will report on this elsewhere.

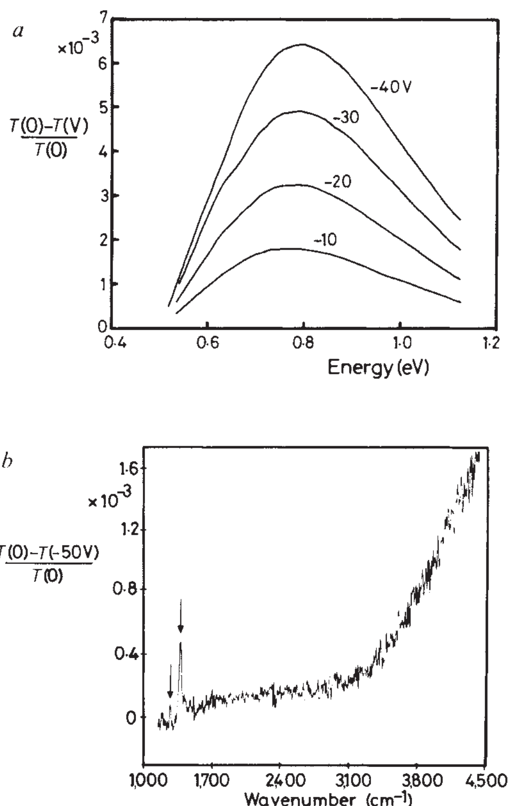

Fig. 7 *a*, Voltage-modulated transmission for a MIS diode, $[T(0)-T(V)]/T(0)$, versus photon energy, for various values of V (all negative with respect to the gate). *b*, Voltage-modulated transmission for a MIS diode, $[T(0)-T(-50V)]/T(0)$, in the spectral range 1,000-4,500 cm^{-1}.

The electro-optic effects we have demonstrated here are large, and there are obvious areas of technology in which these devices may be exploited. Modulation depths, measured here for a single pass of the light beam through the device, can be readily enhanced, either in multiple-reflection structures (Fabry-Perot etalon) or in wave-guided structures in which the light is guided parallel to the active surface of the semiconductor.

We thank British Petroleum PLC for financial support for this work.

Received 6 July; accepted 10 August 1988.

1. *Handbook on Conducting Polymers* (ed. Skotheim, T. J.) (Dekker, New York, 1986).
2. Basescu, N. *et al. Nature* **327**, 403-405 (1987).
3. Grant, P. M., Tani, T., Gill, W. D., Krounbi, M. & Clarke, T. C. *J. appl. Phys.* **52**, 869-873 (1980).
4. Kanicki, J. in *Handbook on Conducting Polymers* (ed. Skotheim, T. J.) 544-660 (Dekker, New York, 1986).
5. Garnier, F. & Horowitz, G. *Synthetic Metals* **18**, 693-698 (1987).
6. Tomozawa, H., Braun, D., Phillips, S., Heeger, A. J. & Kroemer, H. *Synthetic Metals* **22**, 63-69 (1987).
7. Ebisawa, E., Kurokawa, T. & Nara, S. *J. appl. Phys.* **54**, 3255-3260 (1983).
8. Koezuka, H., Tsumura, A. & Ando, T. *Synthetic Metals* **18**, 699-704 (1987).
9. Edwards, J. H. & Feast, W. J. *Polymer Commun.* **21**, 595-597 (1980).
10. Friend, R. H. *et al. Trans. R. Soc.* **A314**, 37-49 (1985).
11. Friend, R. H. *et al. Synthetic Metals* **13**, 101-112 (1986).
12. Bott, D. C. *et al. Synthetic Metals* **14**, 245-269 (1986).
13. Friend, R. H., Bradley, D. D. C., Townsend, P. D. & Bott, D. C. *Synthetic Metals* **17**, 267-272 (1987).
14. Friend, R. H., Bradley, D. D. C. & Townsend, P. D. *J. Phys.* **D20**, 1367-1384 (1987).
15. Friend, R. H., Schaffer, H. E., Heeger, A. J. & Bott, D. C. *J. Phys.* **C20**, 6013-6023 (1987).
16. Su, W. P., Schrieffer, J. R. & Heeger, A. J. *Phys. Rev. Lett.* **42**, 1698-1701 (1979); **B22**, 2099-2111 (1980); erratum, **B28**, 1138 (1983).
17. Rice, M. J. *Phys. Lett.* **71A**, 152-154 (1979).
18. Orenstein, J. in *Handbook on Conducting Polymers* (ed. Skotheim, T. J.) 1297 (Dekker, New York, 1986).
19. Sze, S. M. *Physics of Semiconductor Devices*, 2nd edn (Wiley-Interscience, New York, 1981).
20. Rhoderick, E. M. *Metal-Semiconductor Contacts* (Clarendon Press, Oxford, 1978)
21. Ando, T., Fowler A. B. & Stern, F. *Rev. mod. Phys.* **54**, 437-672 (1982).
22. Horovitz, B. *Solid St. Commun.* **41**, 729-734 (1982).

© 1988 Nature Publishing Group